Journal of Statistical Physics, Vol. 95, Nos. 5/6, 1999

Equations with Singular Diffusivity

R. Kobayashi[1] **and Y. Giga**[2]

Received August 14, 1998; final January 22, 1999

Recently models of faceted crystal growth and of grain boundaries were proposed based on the gradient system with nondifferentiable energy. In this article, we study their most basic forms given by the equations $u_t = (u_x/|u_x|)_x$ and $u_t = (1/a)(au_x/|u_x|)_x$, where both of the related energies include a $|u_x|$ term of power one which is nondifferentiable at $u_x = 0$. The first equation is spatially homogeneous, while the second one is spatially inhomogeneous when a depends on x. These equations naturally express nonlocal interactions through their singular diffusivities (infinitely large diffusion constant), which make the profiles of the solutions completely flat. The mathematical basis for justifying and analyzing these equations is explained, and theoretical and numerical approaches show how the solutions of the equations evolve.

KEY WORDS: Singular diffusivity; faceted growth; grain boundary; extended gradient system.

1. INTRODUCTION

First of all, we would like to state that it is a great honor for us to contribute our article to the special issue of John Cahn's 70th Birthday. As is well-known, he has done a lot of excellent work over a wide range of scientific topics—mathematics, physics and material science, and he is still actively working in these areas. In addition, he has worked as a *bridge* connecting these fields, and we think of this as his greatest contribution to the scientific community. Recently the authors have presented mathematical models of faceted growth of crystals[1] and of the grain boundary,[9] both of which are derived from nondifferentiable energies. These models express non-local interaction in a natural manner using singular diffusivities. We consider that these topics are suitable for the paper dedicated to Dr. Cahn

[1] Research Institute for Electronic Science, Hokkaido University, Sapporo 060, Japan.
[2] Department of Mathematics, Hokkaido University, Sapporo 060, Japan.

0022-4715/99/0600-1187$16.00/0

because they are related to mathematics, physics and material science. Actually, the general mathematical theory provides relevant information for the models, and vice-versa the models motivate the theory. We expect that our work can be one example which enhances the interaction between these areas. However, we were faced with one difficulty. The mathematical basis of our model is unfortunately not well-known to non-mathematicians (at least at this point). In addition, it is usually expressed in a completely mathematical manner, while we recognize that this special issue is not addressed only to mathematicians. Generally speaking, mathematicians always want to be rigorous and as a result tend to write a paper which is hard to understand for those who are not familiar with their jargon. On the other hand the contents themselves often permit an intuitive understanding and are practically useful, and so are ours. Therefore we decided to design our article in a somewhat irregular form. We will explain the mathematical basis of our model in the former part of our article, then state our original results in the latter. Throughout this article, we will try to make the contents as understandable as possible to non-mathematicians. It is not desirable to have barriers between the fields of science, thus our effort to break them is meaningful and fits well with the thought of Dr. Cahn, we believe. Accordingly we do not pursue mathematical rigor, and we refer the readers who are interested in rigorous results to our companion paper.[2]

In this article, we consider the spatially homogeneous energy $E=\int |u_x|\,dx$, and also the inhomogeneous one given by the form $E=\int a(x)\,|u_x|\,dx$. Gradient systems are formally derived from these energies like $u_t=(u_x/|u_x|)_x$ and $u_t=(1/a)(au_x/|u_x|)_x$. The former is closely related to the model of faceted growth and the latter to the one of grain boundary. Although the meaning of the energies are clear, these evolution equations look ambiguous since they include the indeterminate form $u_x/|u_x|$. If u_x never vanishes or vanishes only at the exceptional points, it might be no problem to consider these equations. However, as it will be shown in the following sections, the situation is quite the opposite. In fact, the region where u_x vanishes will increase and finally cover the whole region in the homogeneous case, while in the inhomogeneous case, we are particularly interested in the solutions whose spatial derivative vanishes almost everywhere. Therefore we have to make clear the meaning of the equations and how the solutions behave, especially in the region where u_x vanishes. Fortunately there is a mathematical theory which applies to such situations. We will only state how the theory gives us useful information, especially how it determines the value of the indeterminate form $u_x/|u_x|$ when u_x vanishes. We don't give a rigorous definition of solutions. Instead, we give several examples of solutions which are usually not explicitly written in the mathematical literature.

In Section 2, we will explain the minimum number of basic concepts which are necessary and then we will go ahead utilizing simple examples. In addition, useful general theory will be presented in a brief manner. In Section 3, the spatially homogeneous equation and the theoretical approach to it will be introduced. Up to here we give the explanation of what is well-known or already published, and the rest of this article is devoted to our original results. In the latter half of this section we will demonstrate the numerics of the homogeneous equation. In Section 4, the spatially inhomogeneous equation will be discussed. As previously stated, this equation is related to the grain boundary model introduced in ref. 9. This model includes two variables, one of which is an order parameter of orientation and the other is an angle variable. Although they are, of course, coupled in the model, we will concentrate on the uncoupled form here—i.e., the equation of angle variable assuming another variable is given and fixed. The angle equation itself is mathematically new and worthy of analysis. We found a sufficient condition on $a(x)$ that the piecewise constant structure of solutions are preserved. This is one of the new observations of this paper. Also numerical simulations will be demonstrated.

2. EXTENDED GRADIENT SYSTEMS

In this section, we explain the concept of *subdifferentials* and *extended gradient systems*. Usually the stories related to them are stated in highly mathematical context, and therefore hard to understand for non-mathematicians. However the concept itself is simple and has an easy geometrical interpretation. We begin with simple examples.

2.1. Examples

Let us consider the *convex* function $E(u)$ defined on the real line. A *subdifferential* of E at u is defined as the set of a real number a which satisfies

$$E(u+h)-E(u)\geqslant ah \qquad \text{for arbitrary real number } h \tag{2.1}$$

This set is expressed by $\partial E(u)$.

Example 1. One simplest example of convex function is

$$E(u)=\tfrac{1}{2}u^2 \tag{2.2}$$

What is a subdifferential for this example? The inequality (2.1) means that the line which go through the point $(u, E(u))$ with the slope a is lying

below the graph of $E(u)$. In this example, it is clear that (2.1) holds only when $a = E'(u)$ as shown in Fig. 2.1. Therefore

$$\partial E(u) = \{E'(u)\} = \{u\} \tag{2.3}$$

Generally, subdifferential consists of only one element which is a differential coefficient for the differentiable convex function.

Example 2. One typical example which keeps convexity and breaks differentiability is

$$E(u) = |u| \tag{2.4}$$

It is obvious that $\partial E(u) = \{E'(u)\}$ for non-zero u. Then what is $\partial E(0)$? Considering the geometrical meaning given above, a in (2.1) can be an arbitrary value in the interval $[-1, +1]$ as shown in Fig. 2.2. Then we obtain the subdifferential

$$\partial E(u) = \begin{cases} \{-1\} & u < 0 \\ [-1, +1] & u = 0 \\ \{+1\} & u > 0 \end{cases} \tag{2.5}$$

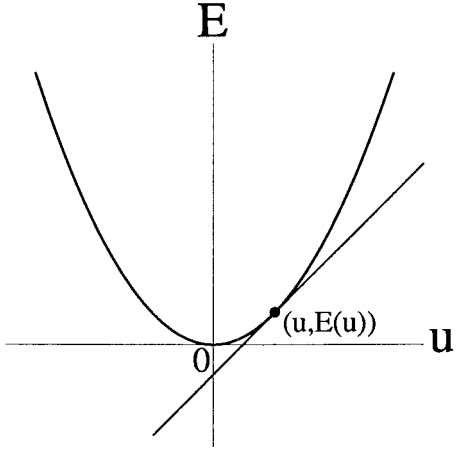

Fig. 2.1. $E(u) = \frac{1}{2}u^2$.

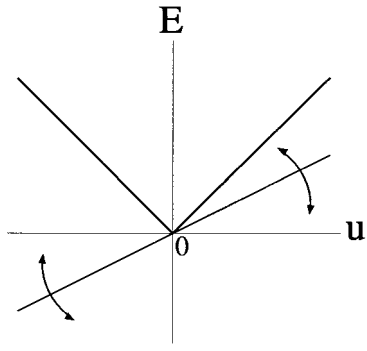

Fig. 2.2. $E(u) = |u|$.

By these examples, it was made clear that the subdifferential is an extended concept of the differential coefficient, which is defined for the convex function. Next, let us consider the *extended gradient system* for the convex energy $E(u)$, which is given by the following form;

$$\frac{du}{dt} \in -\partial E(u) \tag{2.6}$$

You might feel strange to see that the relation in (2.6) is not "$=$" but "$\in$." This is because the subdifferential is not a number but a set of numbers. Also it surely gives an ambiguous impression to the readers since it does not specify the element that is selected as a value of du/dt from the set $-\partial E(u)$ when $\partial E(u)$ has more than one element. Later we will show how this ambiguity is removed by the general theory.

Let us consider the extended gradient system (2.6) using the previous examples.

Example 1. For $E(u) = \frac{1}{2}u^2$, (2.6) simply means

$$\frac{du}{dt} = -u \tag{2.7}$$

since $\partial E(u) = \{E'(u)\} = \{u\}$. If the initial data is given by $u(0) = u_0$, the solution is $u(t) = u_0 e^{-t}$. In this case, there is nothing special and (2.6) gives a usual differential equation. Generally the extended gradient system (2.6) coincides with the usual gradient system $du/dt = -E'(u)$ for differentiable $E(u)$, because $\partial E(u)$ consists of the single element $E'(u)$.

Example 2. For $E(u)=|u|$, the meaning of (2.6) is clear for $u(t)\neq 0$ as follows,

$$\frac{du}{dt}=\begin{cases}-1 & \text{for} \quad u(t)>0\\ +1 & \text{for} \quad u(t)<0\end{cases} \tag{2.8}$$

But, when $u(t)$ vanishes, we know only that $-1\leqslant du/dt\leqslant +1$ holds and don't know how its value is determined.

Here, let us consider the solution with the initial condition $u(0)=u_0>0$. It is easy to solve it until the time $t=u_0$ as shown in Fig. 2.3(a). Then consider what value du/dt should take when $u(t)$ vanishes in order to guarantee that (2.6) can be solved globally (extensible to $t>u_0$). If we take a positive value, the solution try to reflect at $u=0$, but as soon as it becomes positive it must decrease. If a negative value is selected, the solution go through the point $u=0$, but as soon as it becomes negative it must increase. Neither of these selections results in a good behavior. The only natural answer seems to take $du/dt=0$ when $u(t)$ vanishes. Once we determine the rule that $du/dt=0$ for $u(t)=0$, (2.6) always has the global solution for arbitrary initial data u_0, which is given by

$$u(t)=\begin{cases}u_0-\operatorname{sgn}(u_0)\,t & \text{for} \quad 0\leqslant t\leqslant |u_0|\\ 0 & \text{for} \quad t\geqslant |u_0|\end{cases} \tag{2.9}$$

where

$$\operatorname{sgn}(u_0)=\begin{cases}+1 & \text{for} \quad u_0>0\\ 0 & \text{for} \quad u_0=0\\ -1 & \text{for} \quad u_0<0\end{cases} \tag{2.10}$$

The global flow in the $t-u$ plane is indicated in Fig. 2.3(b).

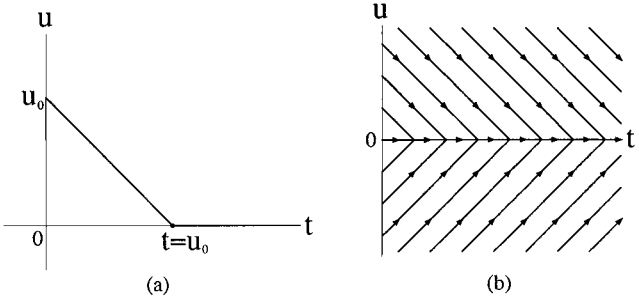

Fig. 2.3. (a) Solution starting from the initial data u_0. (b) Global flow in $t-u$ plane.

Example 2 suggests that there might be some rule for selecting one particular element from the set $\partial E(u(t))$ which assures the global existence of the solution of (2.6). At this point we only refer that the general theory will give an answer to this selection problem. Note that all the solution of Example 2 reach the final state ($u=0$ in this case) within finite time then stop, while the solution of Example 1 takes infinitely long time to vanish.

Next, we extend the concepts defined for the convex functions to convex functionals. Hereafter we consider the functions defined on the interval $I=[0, 1]$, and define the inner product $\langle u, v\rangle$ by

$$\langle u, v\rangle = \int_0^1 u(x)\, v(x)\, dx \tag{2.11}$$

The Dirichlet condition $u(0)=u(1)=0$ will be imposed on the functions unless we particularly refer to the boundary condition. The arguments analogous for the Neumann case. The energy functional $E(u)$ is called *convex* if

$$E((1-t)\, u+tv) \leqslant (1-t)\, E(u)+tE(v) \tag{2.12}$$

holds for arbitrary functions u and v and arbitrary real number t satisfying $0 \leqslant t \leqslant 1$. The subdifferential of E at u is the set of all functions f which satisfies

$$E(u+h)-E(u) \geqslant \langle f, h\rangle \qquad \text{for arbitrary function } h \tag{2.13}$$

This set is expressed by $\partial E(u)$.

We further consider functions $u(x, t)$ with the two independent variables—the space variable x and the time variable t. For each fixed value of t, $u(x, t)$ can be seen as a function of x. Thus we can define the subdifferential $\partial E(u)$ by considering u as a function of x for fixed t. By defining $\partial E(u)$ in such a way, we define the *extended gradient system* by

$$u_t \in -\partial E(u) \tag{2.14}$$

(In this article, the subscripts t and x indicate partial differentiation with respect to the variable t and x, respectively.)

Example 3. At first, we consider the energy

$$E(u) = \int_0^1 \tfrac{1}{2}\, |u_x|^2\, dx \tag{2.15}$$

It is clear that this energy is convex; also it is well-known that the functional derivative is given by

$$\frac{\delta E}{\delta u} = -u_{xx} \tag{2.16}$$

thus the gradient system becomes a basic diffusion equation

$$u_t = u_{xx} \tag{2.17}$$

In this example, the subdifferential of E is given by

$$\partial E(u) = \left\{\frac{\delta E}{\delta u}\right\} = \{-u_{xx}\} \tag{2.18}$$

which means the subdifferential consists of only one element—a functional derivative. This situation corresponds to Example 1. Generally, $\partial E(u) = \{\delta E/\delta u\}$ holds when $\delta E/\delta u$ exists.

Example 4. Let us consider the convex energy

$$E(u) = \int_0^1 |u_x|\, dx \tag{2.19}$$

This example together with its extended gradient system are one of the main concern of our article, thus we devote the entire Section 3 to this example.

Example 5. We can extend Example 4 to a spatially inhomogeneous form such as

$$E(u) = \int_0^1 a(x)\, |u_x|\, dx \tag{2.20}$$

where $a(x)$ is a given positive function. We devote Section 4 to this example.

2.2. General Theory

Before going to the main subjects, we introduce some useful results obtained by the general mathematical theory called *nonlinear semi-group theory* or *variational inequality theory*. It is not our intention here to develope the whole theory properly. We will only state how the general theory relates to our equations. The difficulty is that we don't know how

to handle the ambiguity caused by the fact that the right-hand side of (2.6) or (2.14) is a set. However they are cleared away by the following theorem. Before stating the theorem, we define *canonical restriction* which is a key concept of the theory.

Canonical Restriction. Let us take the nearest element to the origin within the subdifferential $\partial E(u)$. The word "nearest" means smallest in absolute value for the case where $\partial E(u)$ is a subset of the real line. When $\partial E(u)$ consists of of functions, the "nearest" element to the origin is a function f^0 which minimizes $\langle f, f \rangle$ within $\partial E(u)$. In both cases, such a nearest element always exists and is unique, which is guaranteed by the mathematical theory (resulted from the fact that $\partial E(u)$ is a closed convex set). We call this element f^0 a *canonical restriction* of the subdifferential $\partial E(u)$. The following theorem is essential.

Selection Theorem. If we always select the canonical restriction f^0 from $\partial E(u(t))$ and set

$$\frac{du}{dt} = -f^0 \qquad \text{or} \qquad u_t = -f^0 \tag{2.21}$$

the solution $u(t)$ of the extended gradient system (2.6) or (2.14) exists and is uniquely determined by the initial data. There is no other selection which guarantees the global existence of the solution of the extended gradient system. At the point where the differentiability with respect to t is broken, du/dt or u_t stands for the right derivative[3] of u.

It is easily seen that this theorem gives a justification to the intuitive argument for the solution of Example 2. Actually the canonical restriction of $\partial E(0)$ is obviously 0 since the interval $[-1, +1]$ includes the origin. And the derivative always vanishes after the moment when the solution reaches 0. At $t = u_0$, u is not differentiable, and the right derivative there is actually 0. We present one more simple example which is similar to but a little more complicated than Example 2.

Example 6. We take the energy form

$$E(u) = \max(|u|, 2|u| - 1) \tag{2.22}$$

[3] The right derivative is defined by $d^+u/dt(t) = \lim_{\Delta t \to 0+}(u(t+\Delta t) - u(t))/\Delta t$ or $u_{t^+}(x, t) = \lim_{\Delta t \to 0+}(u(x, t+\Delta t) - u(x, t))/\Delta t$. It is, so to say, the change rate to the future.

whose profile is shown in Fig. 2.4(a). It is easy to obtain subdifferentials;

$$\partial E(u) = \begin{cases} \{-2\} & u < -1 \\ [-2, -1] & u = -1 \\ \{-1\} & -1 < u < 0 \\ [-1, +1] & u = 0 \\ \{+1\} & 0 < u < +1 \\ [+1, +2] & u = +1 \\ \{+2\} & u > +1 \end{cases} \tag{2.23}$$

Also we know what values have to be selected from the subdifferentials at the nondifferentiable points $u = \pm 1$ and $u = 0$, when we consider the extended gradient system $du/dt \in -\partial E(u)$. The canonical restrictions of $\partial E(-1)$, $\partial E(0)$ and $\partial E(+1)$ are -1, 0 and $+1$, respectively. The global flow is shown in Fig. 2.4(b), in which we can observe $d^+u/dt = \mp 1$ for $u = \pm 1$ and $du/dt = 0$ for $u = 0$ (or $d^+u/dt = 0$ at the time when u just becomes 0).

Although Examples 2 and 6 seem to be trivial, non-trivial facts will be obtained for Examples 4 and 5 when the theorems are applied to them.

What the selection theorem means is that the canonical restriction actually controls the evolution of the solution. This implies that we can know how the solution will evolve if the canonical restriction can be obtained in some way, which is usually attained by solving a minimization problem. Also it is naturally shown that the energy of the solution of the extended gradient system is non-increasing.

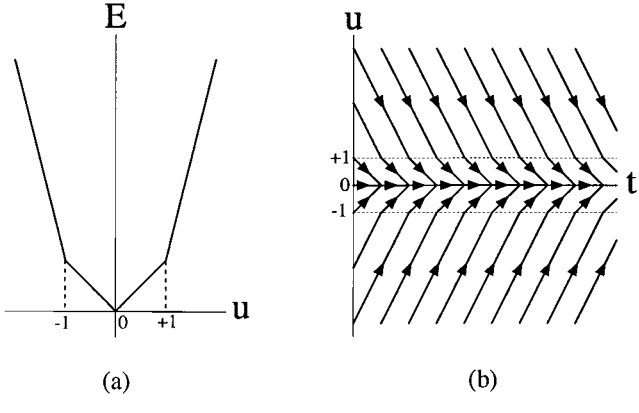

Fig. 2.4. (a) $E(u) = \max(|u|, 2|u| - 1)$. (b) Global flow in $t - u$ plane.

3. SPATIALLY HOMOGENEOUS EQUATION

3.1. Theoretical Approach

In this section we introduce a one dimensional spatially homogeneous equation. We consider the convex energy form given by

$$E(u) = \int_0^1 |u_x|\, dx \tag{3.1}$$

already mentioned in the previous section. First, let us calculate the functional derivative $\delta E/\delta u$ as follows. By ignoring higher order terms in the small perturbation δu, we obtain

$$|(u+\delta u)_x|^2 \simeq |u_x|^2 + 2u_x\,\delta u_x = |u_x|^2 \left(1 + \frac{2u_x\,\delta u_x}{|u_x|^2}\right)$$

thus

$$|(u+\delta u)_x| \simeq |u_x| \left(1 + \frac{u_x\,\delta u_x}{|u_x|^2}\right) = |u_x| + \frac{u_x}{|u_x|}\,\delta u_x$$

By this *formal* calculation, we obtain the *formal* functional derivative

$$\frac{\delta E}{\delta u} = -\left(\frac{u_x}{|u_x|}\right)_x \tag{3.2}$$

and the *formal* gradient system

$$u_t = \left(\frac{u_x}{|u_x|}\right)_x \tag{3.3}$$

But the meaning of the right hand side of (3.2) and (3.3) is not clear in the region where u_x vanishes. Actually the calculation process above doesn't work there.

Our aim here is to demonstrate that such formal expressions make sense under the concept of *subdifferential* and *extended gradient system*. In addition, the general theory not only justifies the equation but also gives us a concrete way of calculating $u_x/|u_x|$ in the region where u_x vanishes. Now we regard the formal equation (3.3) as the extended gradient system $u_t \in -\partial E(u)$. For convenience, we define the three regions D_-, D_0 and D_+ by $D_- = \{u_x < 0\}$, $D_0 = \{u_x = 0\}$ and $D_+ = \{u_x > 0\}$, respectively. Let us define ξ by $\xi = u_x/|u_x|$. Then it is clear that $\xi = -1$ in D_- and $\xi = +1$

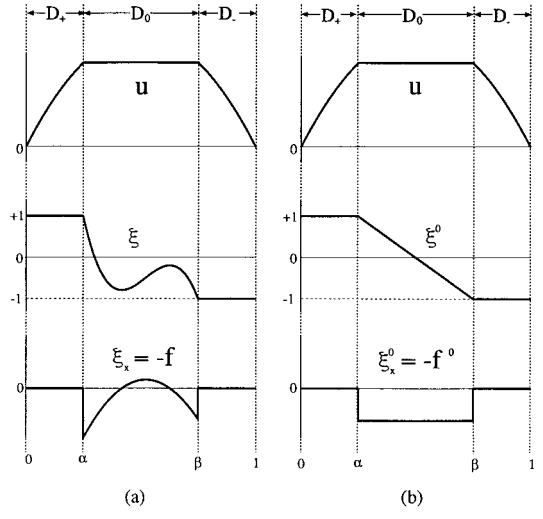

Fig. 3.1. The interval $[0, 1]$ is divided into three intervals $D_+ = [0, \alpha)$, $D_0 = [\alpha, \beta]$ and $D_- = (\beta, 1]$. In D_+, $\xi \equiv +1$ holds, and $\xi \equiv -1$ in D_-. (a) One example of ξ and $\xi_x = -f$ where f belongs to $\partial E(u)$. (b) ξ^0 and $\xi^0_x = -f^0$ where f^0 is a canonical restriction of $\partial E(u)$.

in D_+. The problem is how we determine ξ in D_0. Here we impose the conditions that ξ is continuous in $[0, 1]$ and $-1 \leqslant \xi(x) \leqslant +1$ in D_0.

Note that we have a large degree of freedom to determine the values of $\xi(x)$ in D_0 since the imposed conditions are only the continuity and $-1 \leqslant \xi(x) \leqslant +1$. It is shown mathematically that $f = -\xi_x$ belongs to $\partial E(u)$ if and only if ξ satisfies the above two conditions.[2] A typical example is shown in Fig. 3.1(a).

Here let us recall the *Selection Theorem* which states that the canonical restriction of the subdifferential actually determines the evolution of the solution. Then the question is what is the canonical restriction of $\partial E(u)$. If $f^0 = -\xi^0_x$ is a canonical restriction of $\partial E(u)$, ξ^0 minimizes

$$\int_0^1 f(x)^2 \, dx = \int_\alpha^\beta |\xi_x(x)|^2 \, dx \tag{3.4}$$

under the constraints

$$-1 \leqslant \xi(x) \leqslant +1 \qquad \text{for} \quad \alpha \leqslant x \leqslant \beta$$

$$\xi(\alpha) = +1 \qquad \text{and} \qquad \xi(\beta) = -1$$

by the definition of the canonical restriction. The minimizer is an *affine function* on $[\alpha, \beta]$ which is given by

$$\xi^0(x) = \begin{cases} +1 & \text{for} \quad 0 \leqslant x \leqslant \alpha \\ -\dfrac{2}{\beta - \alpha}(x - \alpha) + 1 & \text{for} \quad \alpha \leqslant x \leqslant \beta \\ -1 & \text{for} \quad \beta \leqslant x \leqslant 1 \end{cases} \tag{3.5}$$

Therefore the canonical restriction f^0 is given by

$$f^0(x) = \begin{cases} 0 & \text{for} \quad 0 \leqslant x < \alpha \\ \dfrac{2}{\beta - \alpha} & \text{for} \quad \alpha \leqslant x \leqslant \beta \\ 0 & \text{for} \quad \beta < x \leqslant 1 \end{cases} \tag{3.6}$$

The profiles of ξ^0 and f^0 are shown in Fig. 3.1(b).

Because $u_t = -f^0 = \xi^0_x$ holds, we naturally regard $u_x/|u_x|$ as ξ^0. By this interpretation for $u_x/|u_x|$, the formal expression $u_t = (u_x/|u_x|)_x$ make sense in the whole region and the ambiguity is now gone.

We have learned how the solution evolves by the extended gradient system. The value of u never changes in both of D_+ and D_- since f^0 vanishes there. Therefore the evolution of the solution is attained only by the change of values in D_0 and the change of D_0 itself. Let us consider the initial data $u_0(x)$ with one flat plateau as shown in Fig. 3.2(a), which is expressed by

$$u_0(x) = \begin{cases} A(x) & \text{for} \quad 0 \leqslant x \leqslant \alpha_0 \\ h_0 & \text{for} \quad \alpha_0 \leqslant x \leqslant \beta_0 \\ B(x) & \text{for} \quad \beta_0 \leqslant x \leqslant 1 \end{cases} \tag{3.7}$$

where $A(x)$ is monotonically increasing and $B(x)$ is monotonically decreasing. We can expect the solution with the form

$$u(x, t) = \begin{cases} A(x) & \text{for} \quad 0 \leqslant x \leqslant \alpha(t) \\ h(t) & \text{for} \quad \alpha(t) \leqslant x \leqslant \beta(t) \\ B(x) & \text{for} \quad \beta(t) \leqslant x \leqslant 1 \end{cases} \tag{3.8}$$

as indicated in Fig. 3.2(b). Since $A(\alpha(t)) = h(t)$ and $B(\beta(t)) = h(t)$ holds and $A(x)$ and $B(x)$ are invertible, we can write $\alpha(t) = A^{-1}(h(t))$ and

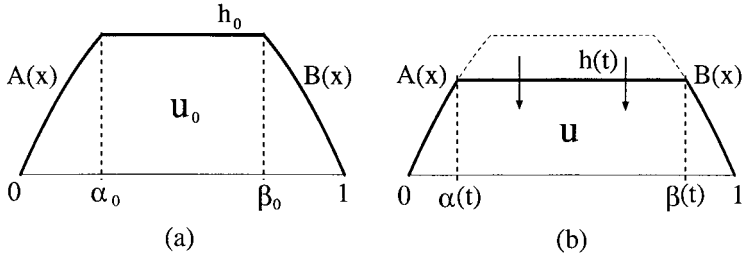

Fig. 3.2. (a) Initial data with one plateau. (b) Evolution of u.

$\beta(t) = B^{-1}(h(t))$. From (3.6), we can see that $h(t)$ is a solution of the following ordinary differential equation

$$\frac{dh}{dt} = -\frac{2}{B^{-1}(h) - A^{-1}(h)} \tag{3.9}$$

with the initial condition $h(0) = h_0$. Once $h(t)$ is known, $\alpha(t)$ and $\beta(t)$ are obtained by substituting $h(t)$ to $\alpha(t) = A^{-1}(h(t))$ and $\beta(t) = B^{-1}(h(t))$, respectively.

Example 7. Let us solve the above problem with the initial data

$$u_0(x) = \begin{cases} x & \text{for} \quad 0 \leqslant x \leqslant \frac{1}{3} \\ \frac{1}{3} & \text{for} \quad \frac{1}{3} \leqslant x \leqslant \frac{2}{3} \\ 1 - x & \text{for} \quad \frac{2}{3} \leqslant x \leqslant 1 \end{cases} \tag{3.10}$$

The equation of $h(t)$ is

$$\frac{dh}{dt} = -\frac{2}{1 - 2h} \tag{3.11}$$

and the initial condition is $h(0) = \frac{1}{3}$. It is easily solved and the solution is

$$h(t) = \begin{cases} \frac{1}{2}(1 - \sqrt{\frac{1}{9} + 8t}) & \text{for} \quad 0 \leqslant t \leqslant \frac{1}{9} \\ 0 & \text{for} \quad t \geqslant \frac{1}{9} \end{cases} \tag{3.12}$$

Thus $\alpha(t) = \frac{1}{2}(1 - \sqrt{\frac{1}{9} + 8t})$ and $\beta(t) = \frac{1}{2}(1 + \sqrt{\frac{1}{9} + 8t})$ until $t = \frac{1}{9}$, and after that time $\alpha(t) \equiv 0$ and $\beta(t) \equiv 1$. Graphs of $\alpha(t)$ and $\beta(t)$ are shown in Fig. 3.3(a).

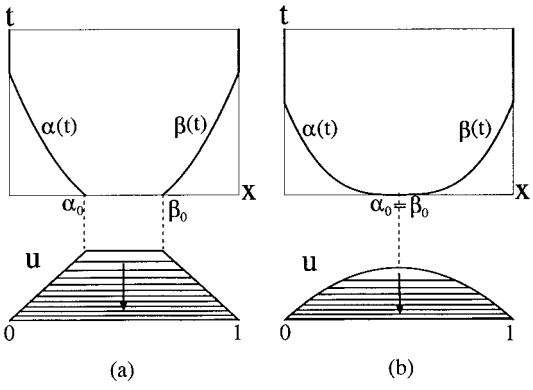

Fig. 3.3. In the lower figures, the solution is displayed every 0.01 time interval. (a) Example 7. (b) Example 8.

Example 8. We can also calculate the solution starting with the initial data

$$u_0(x) = x(1-x) \tag{3.13}$$

In this case, the initial data for $h(t)$, $\alpha(t)$, and $\beta(t)$ are considered to be $h(0) = \frac{1}{4}$ and $\alpha(0) = \beta(0) = \frac{1}{2}$. By following the process of the previous example, we have $h(t) = \frac{1}{4} - (\frac{3}{2}t)^{2/3}$, $\alpha(t) = \frac{1}{2} - (\frac{3}{2}t)^{1/3}$ and $\beta(t) = \frac{1}{2} + (\frac{3}{2}t)^{1/3}$. The solution is shown in Fig. 3.3(b).

In both of Examples 7 and 8, D_0 was surrounded by D_+ on the left side and D_- on the right, and u was decreasing in D_0 and D_0 was growing.

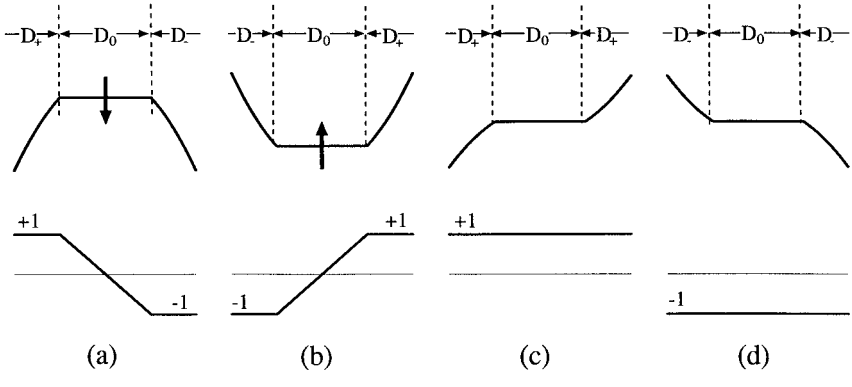

Fig. 3.4. Upper figures show four patterns to sandwich the region D_0. Lower ones are profiles of ξ^0 which corresponds to the canonical restriction f^0 by the relation $f^0 = -\xi^0_x$.

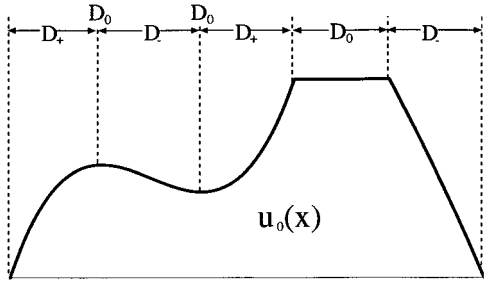

Fig. 3.5. Initial data and the corresponding sequence of regions.

Generally there are four patterns to put D_0 between the two regions as shown in Fig. 3.4. Figure (a) corresponds to Examples 7 and 8. It is obvious that u increases in D_0 and D_0 grows in the case of (b) by the fact that the slope of ξ^0 is positive in D_0. In both of the cases (c) and (d), u does not change at all in the whole region since ξ^0 is constant, and thus D_0 also does not change.

For general initial data, our equation is reduced to a set of ordinary differential equations whose degree of freedom might decrease in time. In fact, we can define the sequence of regions like $\ldots D_{\pm} D_0 D_{\pm} D_0 D_{\pm} D_0 D_{\pm} \ldots$, in which D_0 appears alternately. One example is given in the Fig. 3.5. Note that D_0 consists of a single point if there's an isolated local minimum or local maximum as was seen in Example 8. However such D_0's soon start to grow. Indicating the i-th D_0 at the time t by $[\alpha_i(t), \beta_i(t)]$ and the value of u there by $h_i(t)$, we obtain the following ODE system,

$$\frac{dh_i}{dt} = \frac{2\sigma_i}{A_{i+1/2}^{-1}(h) - A_{i-1/2}^{-1}(h)} \tag{3.14}$$

where $\sigma_i = -1$ if the situation of $[\alpha_i(t), \beta_i(t)]$ is like Fig. 3.4(a), $\sigma_i = +1$ if like (b) and $\sigma_i = 0$ if like (c) or (d), respectively. Also the functions with half-integer subscript are defined by $A_{i+1/2}(x) = u_0(x)$ for $x \in [\beta_i(t), \alpha_{i+1}(t)]$. The region D_+ (or D_-) can disappear along of the evolution of the solution and then the D_0's on its both sides will join, consequently the corresponding degree of freedom in the ODE system decrease. We will demonstrate such a process in our numerical simulations.

3.2. Numerical Simulations

Numerical simulation of (3.3) is not so trivial since it essentially includes the nonlocal interaction, or in other words, singular diffusivities. But the general theory again provides us with a nice theorem for numerics.

Approximation Theorem. If $\tilde{E}(u)$ is an approximation of the energy $E(u)$, then the solution of $u_t \in -\partial \tilde{E}(u)$ approximates the solution of $u_t \in -\partial E(u)$ with the same initial data.

Our plan for designing a numerical scheme is at first taking the differentiable energy $E_\gamma(u)$ approximating $E(u)$ and derive the gradient system $u_t = -(\delta E_\gamma/\delta u)$, and then construct a numerical scheme for this evolution equation. Let us take the energy form with large positive parameter γ by

$$E_\gamma(u) = \int_0^1 \frac{1}{\gamma} \ln \cosh \gamma u_x \, dx \tag{3.15}$$

It is easily seen that it approximates the energy $E(u)$ as shown in Fig. 3.6(a). The corresponding evolution equation is

$$u_t = (\tanh \gamma u_x)_x \tag{3.16}$$

or equivalently

$$u_t = (\chi_\gamma(u_x)\, u_x)_x \tag{3.17}$$

where

$$\chi_\gamma(p) = \frac{\tanh \gamma p}{p} \tag{3.18}$$

Note that this function $\chi_\gamma(p)$ is an approximation of $1/|p|$ for large positive γ as shown in Fig. 3.6(b).

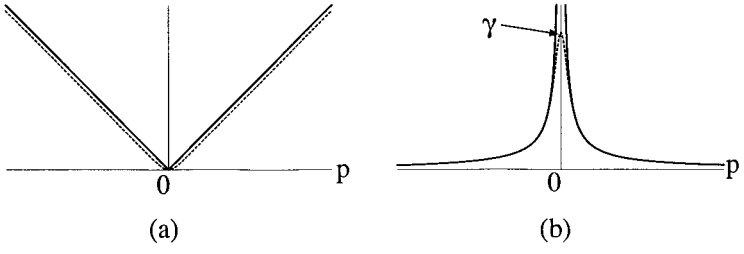

Fig. 3.6. (a) Approximation of $|p|$ (solid curve) by $(\ln \cosh \gamma p)/\gamma$ (dotted curve) as $\gamma \to \infty$. (b) Approximation of $1/|p|$ (solid curve) by $\chi_\gamma(p)$ (dotted curve) whose maximum value is γ.

The form (3.17) was adopted for the numerics since it is a kind of diffusion equation with variable diffusion constant. In order to design a numerical scheme, we definitely have to use an implicit method because the diffusion constant is very large ($\simeq \gamma$) in the region where u_x is close to zero. Our numerical scheme is given by

$$\frac{u_i^n - u_i^{n-1}}{\delta t} = \frac{1}{\delta x}\left[\chi_\gamma\left(\frac{u_{i+1}^{n-1} - u_i^{n-1}}{\delta x}\right)\frac{u_{i+1}^n - u_i^n}{\delta x} - \chi_\gamma\left(\frac{u_i^{n-1} - u_{i-1}^{n-1}}{\delta x}\right)\frac{u_i^n - u_{i-1}^n}{\delta x}\right] \tag{3.19}$$

where δx is a mesh size in space and δt is one in time; i is an index in space and n is one in time.

We will demonstrate several simulations by solving the numerical scheme (3.19). First let us examine Examples 7 and 8 whose exact solution is already obtained.

Examples 7 and 8. The results are shown in Fig. 3.7. Solid curves are the numerical solutions while doted curves are the exact solutions. In the upper figures, the solid curves indicate the boundary between D_0 and $D_\pm$. The profile of the numerical u is just a little bit softened at the

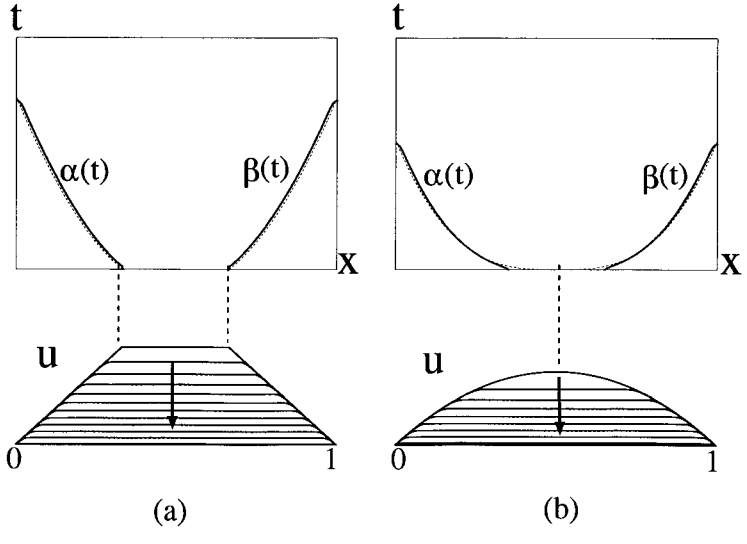

Fig. 3.7. (a) Numerical and exact solution of Example 7. (b) Numerical and exact solution of Example 8. $\gamma = 1000$ in both simulations.

boundary according to the fact that the energy is softened at $u_x = 0$. Therefore it does not matter whether the numerical functions $\alpha(t)$ and $\beta(t)$ approximate the exact $\alpha(t)$ and $\beta(t)$ since the numerical $\alpha(t)$ and $\beta(t)$ depend on how they are calculated from the numerical u. However whether the numerical solution itself approximates the exact solution is important. In the lower figures, the exact solutions are also displayed as dotted curves, but they almost coincide with the numerical solutions within the resolution of graphics.

Example 9. Figure 3.8 shows the evolution of the solution starting from the initial data

$$u_0(x) = \sin \pi x - 0.8 \sin 4\pi x \tag{3.20}$$

In this example D_0's fuse and the whole process is divided into several stages. Snapshots are given in each stage. Standing at some point and observing the state there, we have several modes—increasing, decreasing, freezing, unchanged and locked mode. All the modes except the unchanged mode indicate the state of D_0, i.e., increasing, decreasing and freezing modes correspond to the state shown in Fig. 3.4(b), (a) and (c) + (d), respectively. Locked mode indicates that the value is locked in D_0 by the Dirichlet boundary condition, and unchanged mode is the state in the region $D_{\pm}$. Which mode is selected at the point at the moment depends on the global profile of the solution. For example, the observed history

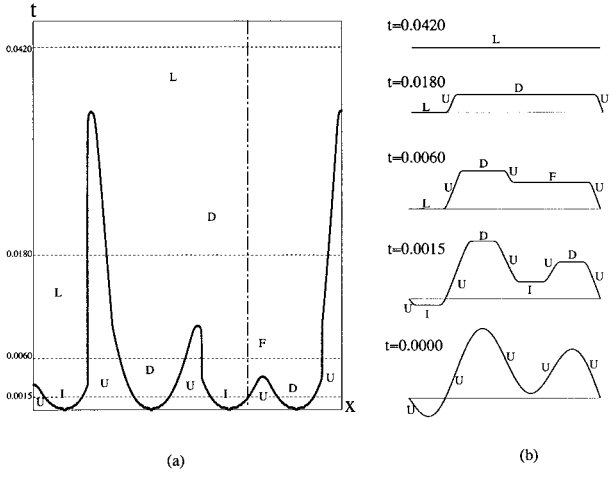

Fig. 3.8. (a) Boundary between D_0 and $D_{\pm}$ are drawn. The characters "I," "D," "F," "L" and "U" indicates increasing, decreasing, freezing, locked and unchanged modes, respectively. (b) Snapshots of the solution.

of the state at the point $x = 0.7$ (vertical dashed line in Fig. 3.8(a)) is "unchanged," "increasing," "freezing," "decreasing" and finally "locked."

So far, we limited our argument to one dimensional space. We can easily extend our method to the multi-dimensional space by replacing the energy form by

$$E(u) = \int_{\Omega} |\nabla u| \, dV \tag{3.21}$$

The derived evolution equation is

$$u_t = \nabla \cdot \left(\frac{\nabla u}{|\nabla u|} \right) \tag{3.22}$$

It is straightforward to construct a numerical scheme similar to the one dimensional one by approximating $1/|\nabla u|$ by $\chi_\gamma(|\nabla u|)$. We demonstrate two simulations in the two dimensional space.

Example 10. First we take the initial data with the simplest profile given by

$$u_0(x, y) = a \sin \pi x \sin \pi y \tag{3.23}$$

on the unit square $[0, 1] \times [0, 1]$. Snapshots are shown in Fig. 3.9. As in the one dimensional computation, the peak is flattened.

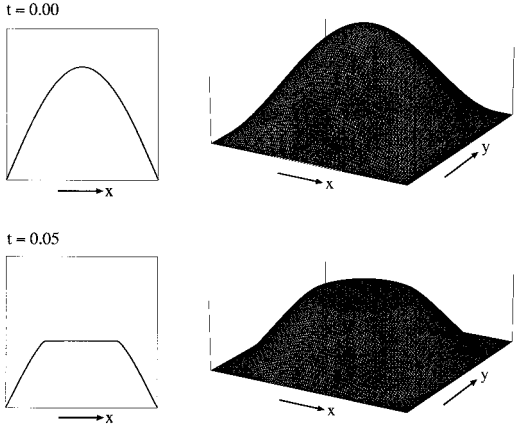

Fig. 3.9. The left panel shows a section of the graph in the right panel along $y = 0.5$. Parameters are given as $a = 1.5$ and $\gamma = 100$.

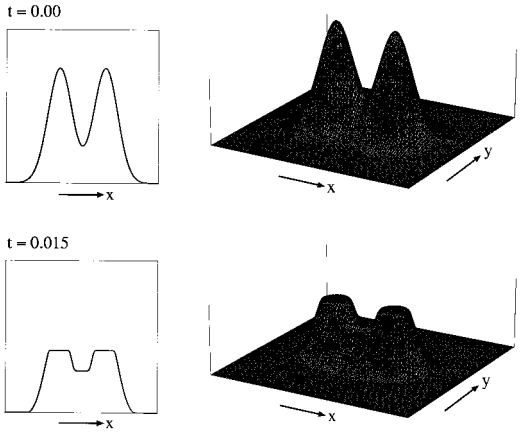

Fig. 3.10. The left panel shows a section of the graph in the right panel along $y = 0.5$. Parameters are given as $a = 1.5$, $m = 3$, $x_1 = 0.35$, $y_1 = 0.5$, $x_2 = 0.65$, $y_2 = 0.5$ and $\gamma = 100$.

Example 11. Let us consider also the mountain-like initial data with two peaks given by

$$u_0(x, y) = ae^{-m^2(r_1^2 + r_2^2)} \tag{3.24}$$

where $r_1^2 = (x - x_1)^2 + (y - y_1)^2$ and $r_2^2 = (x - x_2)^2 + (y - y_2)^2$. Figure 3.10 shows also snapshots of the solution. As is expected, the two peaks are flattened. At the same time, the plateau growing from the saddle point is observed.

4. SPATIALLY INHOMOGENEOUS EQUATIONS

In the phase field type models for grain boundary problem, there is a mathematical difficulty to keep the angle variable constant or almost constant in each grain. One way to solve the problem is to *dig holes* in the energy space according to the finite number of the special grain orientations.[12–16] This obviously breaks the rotational invariance of the model, which is not physically desirable. On the other hand, if no local minimums are assumed in the energy space and if the leading term of the energy with respect to $\nabla\theta$ is $|\nabla\theta|^p$ with $p = 2$ (conventional way), the angle variable is hardly kept constant in each grain, especially without the help of boundary conditions.[10, 11, 17] The following new model equations were derived from the energy including $|\nabla\theta|^p$ with $p = 1$;[9]

$$\begin{aligned}\tau_\eta \eta_t &= v^2 \nabla^2 \eta + 1 - \eta - 2s\eta\,|\nabla\theta| \\ \tau_\theta \theta_t &= \frac{s}{\eta^2} \nabla \cdot \left(\eta^2 \frac{\nabla\theta}{|\nabla\theta|} \right)\end{aligned} \tag{4.1}$$

where η is an order parameter of orientation and θ indicates an angle. It is clear that this model retains a symmetry under rotation since it includes θ only in $\nabla\theta$ form. The basic idea of this model is to keep the angle variable constant by means of *singular diffusivity* in each grain. Then the jump of the angle variable inevitably appears at the grain boundary, consequently we have singular $|\nabla\theta|$. By this singularity, the graph of η is picked downward at the grain boundary, while η prefers the value 1 (ordered state) in bulk. We demonstrate one typical profile of η and θ for the one dimensional problem in Fig. 4.1. The 1st equation in (4.1) is a standard reaction diffusion equation except for the $|\nabla\theta|$ term which is not so difficult to handle. However, the 2nd equation is new and has to be checked mathematically. To begin with we consider that η is a given function depending only on the spatial variable x and examine how the lower equation of (4.1) works in the one dimensional model. The equation which will be studied in this section comes from such a context as stated above.

4.1. Theoretical Approach

In this section, we study the spatially inhomogeneous equation

$$u_t = \frac{1}{a} \left(a \frac{u_x}{|u_x|} \right)_x \tag{4.2}$$

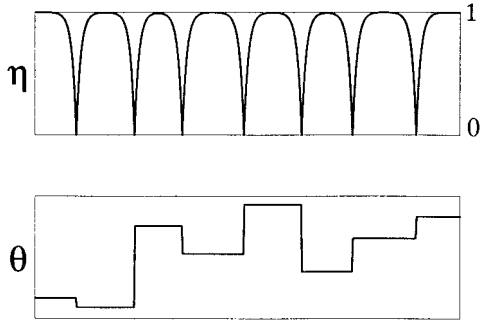

Fig. 4.1. One example of the profiles of η and θ which express multi-grains. The angle variable θ has a discontinuity at several points (grain boundary), and η is nondifferentiable there. Although the local minimums of η look like vanishing, they are small but positive values.

which is derived from the energy form

$$E = \int_0^1 a(x)\,|u_x|\,dx \tag{4.3}$$

The function $a(x)$ corresponds to η^2 in the grain boundary model shown above, which is the reason for the term $1/a$ in the right-hand side of (4.2). At this point, we only assume that $a(x)$ is continuous and positive.

Let us start our discussion from the energetic point of view. At first, we recall the homogeneous equation and consider its boundary conditions. If the Dirichlet boundary conditions $u(0) = u(1) = 0$ are imposed on the homogeneous equation, the final state should be $u \equiv 0$ as was shown in the previous section. If the Neumann boundary conditions $u_x(0) = u_x(1) = 0$ are given, $u \equiv$ constant will be the final state. In both cases, they are obviously global minimizers of the homogeneous energy $E = \int_0^1 |u_x|\,dx$. Then, if we assume the non-uniform Dirichlet boundary conditions, for example, $u(0) = 0$ and $u(1) = 1$, what is a global minimizer? Since $|u_x| \geqslant u_x$ holds,

$$E = \int_0^1 |u_x|\,dx \geqslant \int_0^1 u_x\,dx = u(1) - u(0) = 1 \tag{4.4}$$

It is obvious that the equality holds if u is non-deceasing ($u_x \geqslant 0$); thus every non-decreasing function is a global minimizer. Even a non-decreasing discontinuous function can be regarded as a global minimizer by considering that u_x includes singularities written by Dirac's delta function. In any case, the global minimizer can't be determined uniquely in the homogeneous equation with non-uniform Dirichlet boundary conditions.

Next, let us consider the inhomogeneous energy (4.3) with the same non-uniform Dirichlet boundary conditions as above. If $a(x)$ is a single-well function whose minimum is attained at x_0 as indicated in Fig. 4.2(a), then what is a possible global minimizer of the energy E? From the relation $a(x)\,|u_x| \geqslant a(x_0)\,u_x$, we have

$$E = \int_0^1 a(x)\,|u_x|\,dx \geqslant a(x_0) \int_0^1 u_x\,dx = a(x_0)(u(1) - u(0)) = a(x_0) \tag{4.5}$$

The energy value $a(x_0)$ is actually attained when all the variation of u_x is completely concentrated at the point x_0. Therefore the global minimizer is a step function having a discontinuity only at x_0 as shown in Fig. 4.2(b), and the global minimizer is unique. Of course, the single-well profile of $a(x)$ is not necessary for the uniqueness of the global minimizer. It is sufficient that $a(x)$ attain its minimum at a unique point x_0.

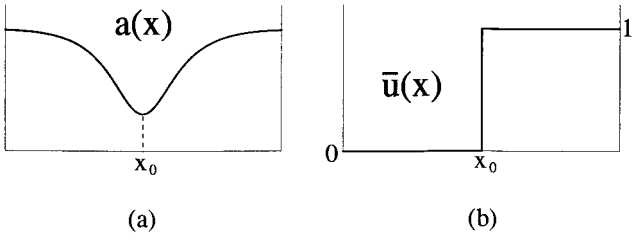

Fig. 4.2. (a) Single-well $a(x)$. (b) Corresponding global minimizer $\bar{u}(x)$.

The example above tells us that the solution quite naturally has a discontinuity since it makes the energy low by concentrating its variation at the point where $a(x)$ is small. Now we restrict our interest to the special form of $a(x)$ and the solutions in connection with the one dimensional grain boundary model. From the argument in the beginning of this section and Fig. 4.1, we extract several properties of η^2 (the profile of η^2 is quite similar to the one of η) and impose them on $a(x)$ as follows;

Conditions on $a(x)$

1. $a(x)$ is continuous and positive on $[0, 1]$,
2. $a(x)$ has local minimums at x_i $(i=1, 2,..., I-1)$, where $0=x_0<x_1<\cdots<x_{I-1}<x_I=1$.
3. $a(x)$ is *concave* on each interval $[x_{i-1}, x_i]$.

According to these conditions, we consider piecewise constant solution u whose typical profile is shown in Fig. 4.3(a). Such solutions are expressed by

$$u=h_i(t) \qquad \text{on each interval } [x_{i-1}, x_i] \tag{4.6}$$

where each $h_i(t)$ is constant for the fixed t and the values of the adjacent intervals are different. Note that it is unknown at this point whether the solution keeps such a piecewise constant profile through the evolution

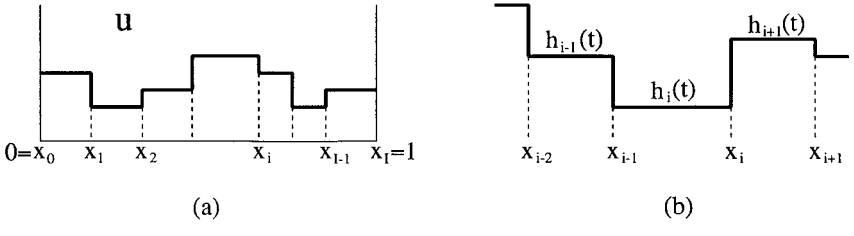

Fig. 4.3. (a) Piecewise constant solution. (b) Values of u in the neighbor of the interval $[x_{i-1}, x_i]$.

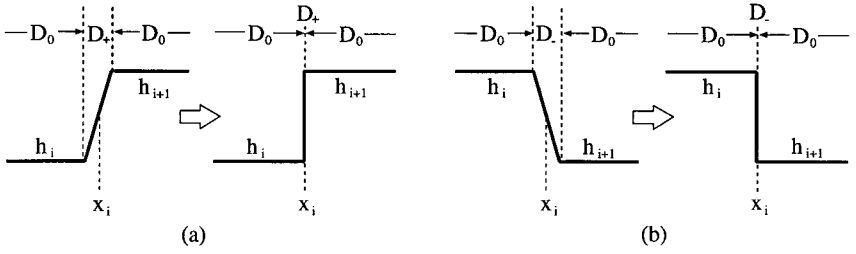

Fig. 4.4. (a) The discontinuous point x_i can be interpreted as a shrunk D_+, thus $\xi(x_i) = +1$. (b) Shrunk D_-, thus $\xi(x_i) = -1$.

process or not. Therefore we have to discuss how such solution is really evolved by the equation (4.2) which is regarded as an extended gradient system.

From here, we start to discuss the subdifferential of such a piecewise constant u and its canonical restriction. Thus, we fix the variable t and forget the dependence on t for a while. Let us set $\xi = u_x/|u_x|$ for the piecewise constant u as we did in the previous section. In contrast to the previous case, there is no point where the value of ξ can be determined at a glance, because either $u_x = 0$ or "u is discontinuous" happens in the whole region. However, it is plausible to set $\xi(x_i) = +1$ when $h_i < h_{i+1}$, because u can be interpreted as a limit of the piecewise linear function which is continuous and increasing in the vicinity of x_i as shown in Fig. 4.4. Similarly we can set $\xi(x_i) = -1$ if $h_i > h_{i+1}$. In addition, we impose the conditions that ξ is continuous and satisfies $-1 \leqslant \xi \leqslant +1$ on $[0, 1]$. Then, it is proved[(2)] that the function f which is defined by $f = -(1/a)(a\xi)_x$ belongs to the subdifferential $\partial E(u)$.[4] What we really need is, of course, the canonical restriction f^0 of $\partial E(u)$ in order to know how the solution evolves. It is also proved[(2)] that the canonical restriction f^0 is selected from such a set of f's as described above by the following property;

Selection Condition. f^0 is constant on each interval $[x_{i-1}, x_i]$.

By this characterization of f^0, we can calculate f^0 and the corresponding ξ^0. In fact, by setting

$$f^0 = -C_i \qquad \text{on } [x_{i-1}, x_i] \tag{4.7}$$

where C_i is a constant, we have

$$(a\xi^0)_x = C_i a \qquad \text{on } [x_{i-1}, x_i] \tag{4.8}$$

[4] Note that the inner product $\langle \cdot, \cdot \rangle_a$ defined by $\langle u, v \rangle_a = \int_0^1 a(x)\, u(x)\, v(x)\, dx$ is adopted in the inhomogeneous case. Thus $\partial E(u)$ and f^0 are defined using this inner product.

Integrating (4.8) from x_{i-1} to x_i, the constant C_i is determined as follows;

$$C_i = \frac{a(x_i)\,\xi^0(x_i) - a(x_{i-1})\,\xi^0(x_{i-1})}{\int_{x_{i-1}}^{x_i} a(x)\,dx} \tag{4.9}$$

Note that (4.9) holds for $i = 2, 3, \ldots, I-1$, and $C_0 = C_I = 0$ must hold since the values are locked by the Dirichlet conditions in the intervals $[x_0, x_1]$ and $[x_{I-1}, x_I]$. Again by integrating (4.8) from x_{i-1} to x, we obtain

$$\xi^0(x) = \frac{1}{a(x)}\left[a(x_{i-1})\,\xi^0(\xi_{i-1}) + C_i \int_{x_{i-1}}^{x} a(\tilde{x})\,d\tilde{x} \right] \tag{4.10}$$

on the interval $[x_{i-1}, x_i]$.

Now we have the local evolution rule, and let us come back to the time dependent problem. Since the change rate of u is constant on each interval, the piecewise constant profile of u is kept in the evolution process. Thus the solution permits an expression (4.6), if the initial data has a piecewise constant profile whose discontinuous points coincide to the local minimum points of $a(x)$. The evolution rule is written as follows;

$$\frac{dh_i}{dt} = \frac{a(x_i)\,\mathrm{sgn}(h_{i+1} - h_i) - a(x_{i-1})\,\mathrm{sgn}(h_i - h_{i-1})}{\int_{x_{i-1}}^{x_i} a(x)\,dx} \tag{4.11}$$

for $i = 2, 3, \ldots, I-1$. For the intervals of both ends,

$$h_1(t) \equiv \bar{u}_{\mathrm{left}} \qquad \text{and} \qquad h_I(t) \equiv \bar{u}_{\mathrm{right}} \tag{4.12}$$

where $\bar{u}_{\mathrm{left}}$ and $\bar{u}_{\mathrm{right}}$ are constants given by the Dirichlet boundary conditions. If the Neumann boundary conditions $u_x(0, t) = u_x(1, t) = 0$ are imposed,

$$\frac{dh_1}{dt} = \frac{a(x_1)\,\mathrm{sgn}(h_2 - h_1)}{\int_{x_0}^{x_1} a(x)\,dx} \qquad \text{and} \qquad \frac{dh_I}{dt} = -\frac{a(x_{I-1})\,\mathrm{sgn}(h_I - h_{I-1})}{\int_{x_{I-1}}^{x_I} a(x)\,dx} \tag{4.13}$$

hold. Note that the change rate of $h_i(t)$ is constant in t, thus $h_i(t)$ varies linearly in t as long as the relations between $h_i(t)$ and $h_{i+1}(t)$ and between $h_i(t)$ and $h_{i-1}(t)$ are kept. We should not forget that this evolution rule holds until the first moment when the values of the solution on some adjacent intervals coincide. After the coincidence, what will happen? This problem is not so easy to answer and we will study it in the following example and in the next subsection.

Example 12. Let us take $x_0 = 0$, $x_1 = \frac{1}{4}$, $x_2 = \frac{3}{4}$ and $x_3 = 1$, and define the piecewise linear function $a(x)$ by connecting the five points

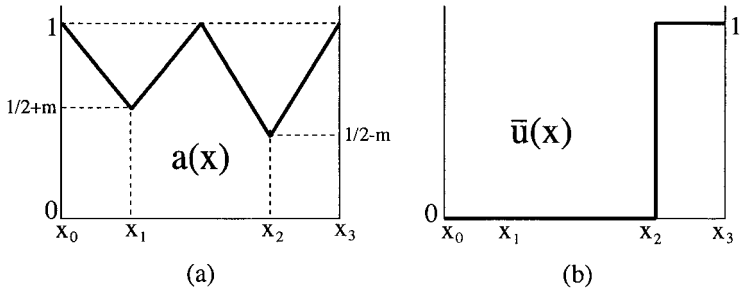

Fig. 4.5. (a) Piecewise linear $a(x)$. (b) Corresponding global minimizer $\bar{u}(x)$.

$(x_0, 1)$, $(x_1, 1/2+m)$, $(1/2, 1)$, $(x_2, 1/2-m)$ and $(x_3, 1)$ in this order as indicated in Fig. 4.5(a). The constant m is assumed to satisfy $0<m<\frac{1}{2}$, thus $a(x)$ satisfies all the conditions required. Also $a(x)$ attains its global minimum at $x=x_2$. We take the piecewise constant initial data u_0 and analyze how it evolves. In this example, we impose the Dirichlet conditions $u(0, t)=0$ and $u(1, t)=1$, thus the values on $[x_0, x_1]$ and $[x_2, x_3]$ are locked. By taking the initial data compatible with the boundary conditions, we have $h_1(t)\equiv 0$ and $h_3(t)\equiv 1$. Therefore the solution u is expressed only by $h_2(t)$. As shown in Fig. 4.6, the initial data u_0 is classified into the three patterns; $h_2(0)<0$, $0<h_2(0)<1$ and $h_2(t)>1$. By the evolution rule (4.11), we have

$$\frac{dh_2}{dt}=\frac{8}{3}\left[\left(\frac{1}{2}-m\right)\operatorname{sgn}(1-h_2(t))-\left(\frac{1}{2}+m\right)\operatorname{sgn}(h_2(t))\right] \tag{4.14}$$

If $h_2(0)<0$, $dh_2/dt=\frac{8}{3}$ holds until the time when $h_2(t)$ reaches to 0, then u becomes a global minimizer and stops. If $0<h_2(0)<1$, $dh_2/dt=-\frac{16}{3}m$ holds until the time when $h(t)$ reaches to 0, then u becomes a global minimizer and does not change anymore. If $h_2(0)>1$, $dh_2/dt=-\frac{8}{3}$ holds until

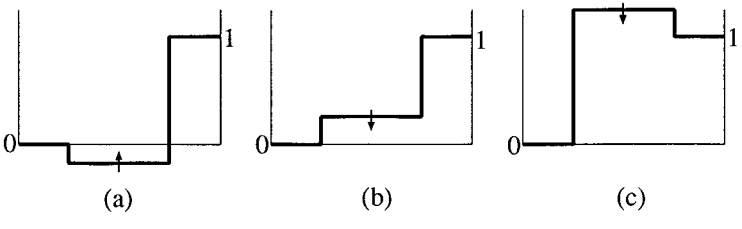

Fig. 4.6. Three patterns of the initial data and the direction of elevator move of the central part. (a) $h_2(0)<0$, (b) $0<h_2(0)<1$, (c) $h_2(0)>1$.

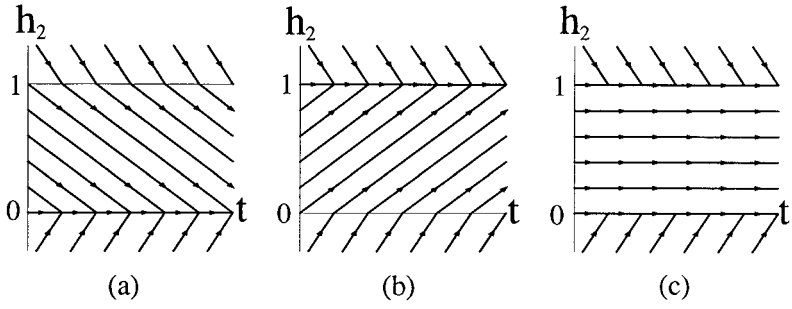

Fig. 4.7. Global flow in $t-h_2$ plane. (a) $m>0$, (b) $m<0$, (c) $m=0$.

the time when $h(t)$ reaches to 1. Now we encounter the problem whether $h_2(t)$ will stop at the value 1 or continue to decrease. In this case, it is not so difficult to judge which will happen, since it is more advantageous energetically to continue decreasing. Therefore the solution eventually satisfies $0<h_2(t)<1$ and follows the new rate $dh_2/dt=-\frac{16}{3}m$, and finally reaches the state 0. In any case, the solution arrives at the global minimizer $h_2=0$ in finite time. The global flow in $t-h_2$ plane is indicated in Fig. 4.7(a). Figure 4.7(b) shows the flow for $m<0$, in which the global minimizer is $h_2=1$. For $m=0$, arbitrary h_2 which satisfies $0\leqslant h_2\leqslant 1$ is a global minimizer. In the next subsection, more complicated examples will be examined by numerical simulations.

Grain Boundary Model. Before going to the next subsection, we apply our results to the grain boundary model (4.1).[9] In this model, the ordering variable η is approximately expressed by $\eta\simeq 1-(1-\eta(x_0))e^{-|x-x_0|/v}$ where x_0 indicates a grain boundary point, as long as the grain boundary point is well isolated from another ones. Under the assumption $s\gg v$ and the angles in the grains on the both sides are not so close, the value $\eta(x_0)$ is also approximated by $\eta(x_0)\simeq v/(s\,\Delta\theta)$ where $\Delta\theta$ is an absolute value of the jump of θ at the grain boundary point. Here, let us consider a situation similar to Example 12 as shown in Fig. 4.8, in which the two grain boundary points x_- and x_+ are located in well-separated positions with the distance l ($l\gg v$). The angle variables in the grains on the both sides are locked by the boundary conditions, say θ_- on the left grain and θ_+ on the right, and we indicate the value of the angle variable in the central grain by $\theta_0(t)$. Since the movement of the positions of the grain boundary makes almost no difference to the energy as long as the two grain boundaries are apart, the evolution of the solution is attained by the *elevator motion* of the angle variable $\theta_0(t)$ with fixed positions of the

grain boundary points. Thus our concern is how $\theta_0(t)$ evolves. Using (4.11) and scaling the time variable appropriately, we obtain

$$\tau_\theta \frac{d\theta_0}{dt} = s \frac{\eta(x_+)^2 \operatorname{sgn}(\theta_+ - \theta_0) - \eta(x_-)^2 \operatorname{sgn}(\theta_0 - \theta_-)}{\int_{x_-}^{x_+} \eta(x)^2 \, dx} \tag{4.15}$$

Considering the form of η and the relation $l \gg v$, we have $\int_{x_-}^{x_+} \eta(x)^2 \, dx \simeq l$. Let us assume $\theta_- < \theta_+$ and examine for the three cases; $\theta_0(t) < \theta_-$, $\theta_- < \theta_0(t) < \theta_+$ and $\theta_0(t) > \theta_+$. In the first case,

$$\tau_\theta \frac{d\theta_0}{dt} \simeq \frac{v}{l}\frac{v}{s}\left(\frac{1}{(\theta_+ - \theta_0)^2} + \frac{1}{(\theta_- - \theta_0)^2}\right) \tag{4.16}$$

Similarly in the third case,

$$\tau_\theta \frac{d\theta_0}{dt} \simeq -\frac{v}{l}\frac{v}{s}\left(\frac{1}{(\theta_0 - \theta_0)^2} + \frac{1}{(\theta_0 - \theta_-)^2}\right) \tag{4.17}$$

In the second case,

$$\begin{aligned} \tau_\theta \frac{d\theta_0}{dt} &\simeq \frac{v}{l}\frac{v}{s}\left(\frac{1}{(\theta_+ - \theta_0)^2} - \frac{1}{(\theta_0 - \theta_-)^2}\right) \\ &= \frac{v}{l}\frac{v}{s}\frac{2(\theta_+ - \theta_-)}{(\theta_0 - \theta_-)^2 (\theta_+ - \theta_0)^2}\left(\theta_0 - \frac{\theta_+ + \theta_-}{2}\right) \end{aligned} \tag{4.18}$$

These formulas mean that $\theta_0(t)$ approaches the one of the angles θ_- and θ_+ which is closer to $\theta_0(t)$. In this model, once the angles of adjacent grains coincide, the corresponding local minimum of η disappears, which is a difference from the equation with fixed $a(x)$.

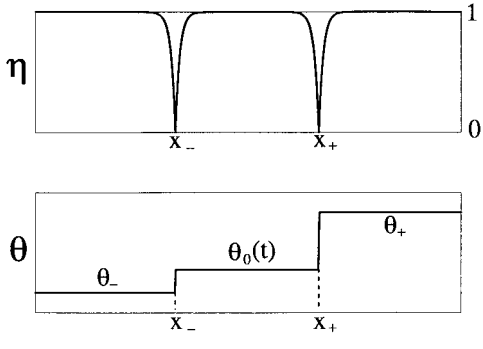

Fig. 4.8. Sandwiched grain.

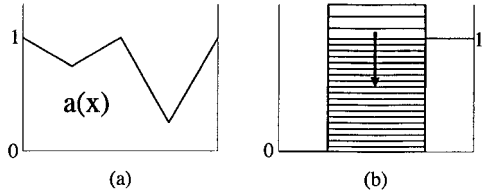

Fig. 4.9. (a) Profile of $a(x)$ for $m=0.25$. (b) Numerical solution which started from $h_2(0)=1.3$.

4.2. Numerical Simulations

A numerical scheme for (4.2) is constructed by following the same idea with the one introduced in the previous section. We first approximate the energy (4.3) by

$$E_\gamma(u)=\int_0^1 a(x)\frac{1}{\gamma}\ln\cosh \gamma u_x\,dx \tag{4.19}$$

with a large positive parameter γ, and derive the gradient system of (4.19) as follows;

$$u_t=\frac{1}{a}(a\chi_\gamma(u_x)\,u_x)_x \tag{4.20}$$

where χ_γ is defined by (3.18). Then our numerical scheme is expressed by

$$\begin{aligned}\frac{u_i^n-u_i^{n-1}}{\delta t}=\frac{1}{a_i}\frac{1}{\delta x}\Bigg[&a_{i+1/2}\chi_\gamma\left(\frac{u_{i+1}^{n-1}-u_i^{n-1}}{\delta x}\right)\frac{u_{i+1}^n-u_i^n}{\delta x}\\&-a_{i-1/2}\chi_\gamma\left(\frac{u_i^{n-1}-u_{i-1}^{n-1}}{\delta x}\right)\frac{u_i^n-u_{i-1}^n}{\delta x}\Bigg]\end{aligned} \tag{4.21}$$

where $a_{i\pm 1/2}$ are evaluated at half mesh points.

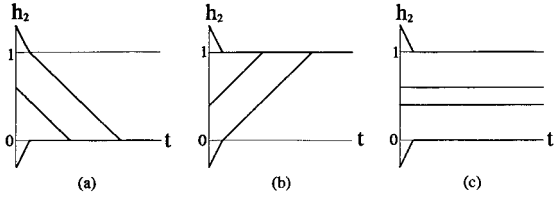

Fig. 4.10. Numerical solution is drawn by plotting $u(1/2, t)$ using solid curve, while exact ones by dotted line which are hardly seen. (a) $m=0.25$ and $h_2(0)=-0.3$, 0.6, 1.3, (b) $m=-0.25$ and $h_2(0)=-0.3$, 0.4, 1.3, (c) $m=0.0$ and $h_2(0)=-0.3$, 0.4, 0.6, 1.3.

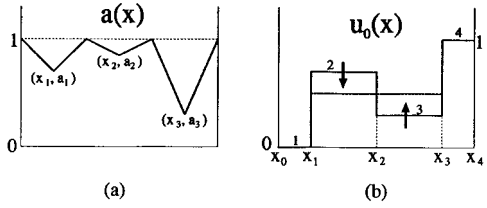

Fig. 4.11. (a) Profile of $a(x)$ for $a_1 = 0.7$, $a_2 = 0.85$ and $a_3 = 0.3$. (b) Initial data and the evolution in the first stage, where $h_2(0) = 0.7$ and $h_3(0) = 0.3$. Small numbers are indicators of the interval which equals the subscript i of $h_i(t)$.

Example 12. Since the exact solution is known for the Example 12, it can be used as a test problem for our numerical scheme (4.21). One simulated solution is shown in Fig. 4.9(b). The discontinuity of the exact solution is well simulated within the mesh size, and the flatness on each interval is also complete. We also show the $t - h_2$ plots for several initial data together with the exact solution for positive, negative and vanishing m in Fig. 4.10. Numerical solutions almost coincide with the exact ones within the resolution of the graph.

Example 13. In this example, we consider a little more complicated case. The function $a(x)$ is given by connecting $(0, 1)$, $(1/6, a_1)$, $(2/6, 1)$, $(3/6, a_2)$, $(4/6, 1)$, $(5/6, a_3)$ and $(1, 1)$ in this order as shown in Fig. 4.11(a). Here a_1 and a_3 are assumed to satisfy the relation $0 < a_3 < a_1 < 1$, and we Control the parameter a_2 between 0 and 1. The points determining the division to the intervals are given as follows; $x_0 = 0$, $x_1 = \frac{1}{6}$, $x_2 = \frac{3}{6}$, $x_3 = \frac{5}{6}$ and $x_4 = 1$. We take the initial data which satisfies $0 < h_3(0) < h_2(0) < 1$ as shown in Fig. 4.11(b). It is a direct result of (4.11) that

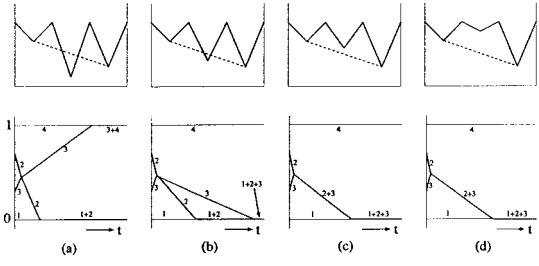

Fig. 4.12. Upper panels are graphs of $a(x)$, and lower ones show $u(1/3, t)$ plotted by solid curve and $u(2/3, t)$ by dotted curve. Small numbers correspond to the ones in Fig. 4.11. The notation using $+$, for example "$2 + 3$," means that the values on the adjacent intervals keep their equality after their coincidence. (a) $a_2 = 0.15$, (b) $a_2 = 0.40$, (c) $a_2 = 0.60$, (d) $a_2 = 0.85$.

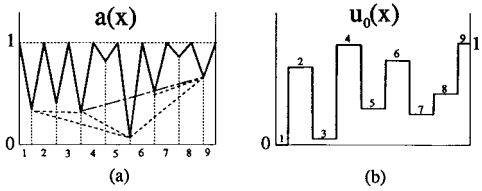

Fig. 4.13. (a) Solid line indicates a profile of $a(x)$. Short dashed lines connecting the local minimums of $a(x)$ are corresponding to the fusion of the two orbits in Fig. 4.13, and dashed line connecting (x_3, a_3) and (x_8, a_8) corresponds to the crossing of the two orbits ("4 + 5" and "6 + 7 + 8"). (b) Initial data $u_0(x)$. Small numbers are indicators of the intervals which equal to the subscript i of h_i.

$h_2(t)$ decreases and $h_3(t)$ increases until they coincide whatever a_2 is. Then the problem is what will happen next. Figure 4.12 shows the evolution of $h_2(t)$ and $h_3(t)$ for the several values of a_2. Our observation from these results is that $h_2(t)$ and $h_3(t)$ go together after their coincidence if (x_2, a_2) is located above the line which connects (x_1, a_1) and (x_3, a_3) (indicated by short dashed line in upper panels of Fig. 4.12). It is also observed that $h_2(t)$ and $h_3(t)$ go apart after the coincidence if (x_2, a_2) is located below the short dashed line. We will examine this hypothesis in the next example.

Example 14. We increase the number of intervals and set the function $a(x)$ and the initial data $u_0(x)$ by using random numbers as shown in Fig. 4.13. Local minimum points of $a(x)$ are (x_1, a_1), (x_2, a_2),..., (x_8, a_8) in this order from the left end. The result of the simulation is demonstrated in Fig. 4.14. Merging of the two orbits happen sequentially. At first, the orbits "7" and "8" make a pair, and next "4" and "5," then "6" and "7 + 8" follows. Note that our hypothesis holds in these merging, for example (x_7, a_7) is located *above* the line connecting (x_6, a_6) and (x_8, a_8) as

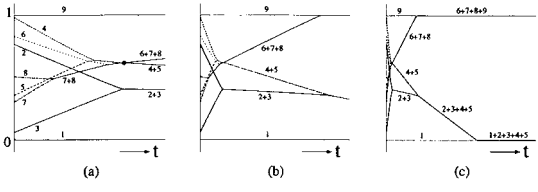

Fig. 4.14. Numerical solution is indicated by plotting the values at the center of the intervals. Small numbers correspond to the ones in Fig. 4.13. Three panels are drawn by the same simulation where (a) shows the early stage ($t = 0 \sim 0.06$), (b) does the intermediate one ($t = 0 \sim 0.3$) and (c) does the last ($t = 0 \sim 1.2$). The crossing between "4 + 5" and "6 + 7 + 8" is indicated by the small circle in the panel (a). Note that the crossing between orbits of non-adjacent pairs has no meaning.

indicated Fig. 4.13(a), and so on. Similarly, "2" and "3" go together after their coincidence. Just after that, the values of "4 + 5" and "6 + 7 + 8" coincide. They do not make a pair and go apart, since (x_5, a_5) lies *below* the line connecting (x_3, a_3) and (x_8, a_8). Then one more merging between "2 + 3" and "4 + 5" occurs, and finally "2 + 3 + 4 + 5" and "6 + 7 + 8" are locked to "1" and "9" respectively, and the solution reaches to the global minimum. We made several simulations by changing the random number sequence, and we observed that the equation in this example has the following properties.

1. For arbitrary initial data, the solution reaches the global minimizer in a finite time.

2. When two orbits come across (each of them may be composed of several orbits already), whether they merge or not is determined as follows. Let x_l and x_r be x-coordinate of the left and right ends of the region consists of all the related intervals, and x_b a boundary point between the two regions corresponding to the two orbits. The two orbits merge if and only if the point $(x_b, a(x_b))$ is located *above* the line connecting $(x_l, a(x_l))$ and $(x_r, a(x_r))$.

For more general $a(x)$, it turns out that the condition which guarantees the merging of orbits is more complicated than the above observation. We shall study the precise condition in ref. 2.

APPENDIX. BRIEF MATHEMATICAL BACKGROUND FOR THE SECTIONS 2 AND 3

We present a mathematical background of the contents of the Section 2 and 3 for those who are interested in it. The theory of nonlinear semigroup theory was initiated by Y. Komura[3] and developed by many mathematicians for many years; see the book of V. Barbu[6] for details which provides a mathematical formulation of various important problems including Stefan problem and Hele-Shaw problem; see also the book of A. Visintin[8] for these applications. The theory provides a unique global-in-time solution of the initial value problem for the extended gradient system. However, since the calculation of the subdifferential is not easy, the explicit shape of the solution has not been very well studied. Several years ago J. Taylor[4] and independently S. Angenent and M. Gurtin[7] formulated the motion of faceted phase boundaries by a singular interfacial energy called crystalline energy. In some special geometries their explicit solutions turn out to coincide with the solution of nonlinear semigroup theory if the equation is an extended gradient system. However, in general

the equation is not an extended gradient system, so another approach is necessary. based on the order preserving structure of the problem, a new approach was established by M.-H. Giga and Y. Giga[1] for the spatially homogeneous problem for evolving graphs. For the background of growth of faceted curves and for the theoretical development as well as the example (3.8), see ref. 1. This method provides a stronger approximation theorem than the nonlinear semigroup approach in L^2 spaces. By the way, the theory developed by ref. 5 is along the lines of the nonlinear semigroup theory. It concerns the equation $u_t = \nabla \cdot (\nabla u/|\nabla u|)$ and includes examples of solution (3.8).

REFERENCES

1. M.-H. Giga and Y. Giga, *Arch. Rational Mech. Anal.* **141**:117 (1998).
2. M.-H. Giga, Y. Giga and R. Kobayashi, Hokkaido Univ. Preprint Ser. in Math., #461 (1999).
3. Y. Komura, *J. Math. Soc. Japan* **19**:493 (1967).
4. J. E. Taylor, *Proc. Symp. Pure Math.* **54**:417 (1993).
5. R. Hardt and X. Zhou, *Commun. in Partial Differential Equations* **19**:1879 (1994).
6. V. Barbu, *Nonlinear Semigroups and Differential Equations in Banach Spaces* (Noordhoff, Groninger, 1976).
7. S. G. Angenent and M. E. Gurtin, *Arch. Rat. Mech. Anal.* **108**:323 (1989).
8. A. Visintin, *Models of Phase Transitions* (Birkhäuser, 1996).
9. R. Kobayashi, J. A. Warren, and W. C. Carter, Hokkaido Univ. Preprint Ser. in Math., #422 (1998).
10. R. Kobayashi, J. A. Warren, and W. C. Carter, *Physica D* **119**:415 (1998).
11. J. A. Warren, W. C. Carter, and R. Kobayashi, *Physica A* **261**:159 (1998).
12. B. Morin, K. R. Elder, M. Sutton, and M. Grant, *Phys. Rev. Lett.* **75**:2156 (1995).
13. J. A. Warren, W. C. Carter, and A. R. Roosen, unpublished (1995).
14. Long-Qing Chen and Wei Yang, *Phys. Rev. B* **50**:15752 (1994).
15. M. T. Lusk, submitted to *Physical Review B* (1998).
16. I. Steinbach, F. Pezzolla, B. Nestler, M. BeeBelber, R. Prieler, G. J. Schmitz, and J. L. L. Rezende, *Physica D* **94**:135 (1996).
17. M. T. Lusk, *Proc. Royal Soc. London A* **455**:677 (1999).